

DiPA: Diverse and Probabilistically Accurate Interactive Prediction

Anthony Knittel¹, Majd Hawasly¹, Stefano V. Albrecht^{1,2}, John Redford¹, Subramanian Ramamoorthy^{1,2}

Abstract—Accurate prediction is important for operating an autonomous vehicle in interactive scenarios. Previous interactive predictors have used closest-mode evaluations, which test if one of a set of predictions covers the ground-truth, but not if additional unlikely predictions are made. The presence of unlikely predictions can interfere with planning, by indicating conflict with the ego plan when it is not likely to occur. Closest-mode evaluations are not sufficient for showing a predictor is useful, an effective predictor also needs to accurately estimate mode probabilities, and to be evaluated using probabilistic measures. These two evaluation approaches, eg. predicted-mode RMS and minADE/FDE, are analogous to precision and recall in binary classification, and there is a challenging trade-off between prediction strategies for each. We present DiPA, a method for producing diverse predictions while also capturing accurate probabilistic estimates. DiPA uses a flexible representation that captures interactions in widely varying road topologies, and uses a novel training regime for a Gaussian Mixture Model that supports diversity of predicted modes, along with accurate spatial distribution and mode probability estimates. DiPA achieves state-of-the-art performance on INTERACTION and NGSIM, and improves over a baseline (MFP) when both closest-mode and probabilistic evaluations are used at the same time.

I. INTRODUCTION

Prediction of the future motion of surrounding road users is essential for the safe operation of an autonomous vehicle. In order to support planning, a predictor needs to estimate the future states of the surrounding road users based on observations of their recent history, and to estimate the risk of conflict for possible ego actions. Road scenarios such as intersections, merges and roundabouts require significant interaction between agents in the scene, where agent behaviour is influenced by the presence of nearby agents, as well as reactions to actions that other agents take. The INTERACTION dataset [1] covers such interactive scenarios.

Existing methods that have used the INTERACTION dataset such as [2], [3], [4] are examples of predictors that are able to capture ground-truth behaviours with one of a set of predicted trajectory modes, as evaluated using minimum average- or final-displacement error (minADE/FDE) and miss-rate (MR) (see Section IV-B for a definition). These measures compare the closest predicted mode with the ground-truth. A limitation of these evaluations is that additional predicted modes (other than the closest) do not affect scoring, thus no assessment takes place of whether the model is also predicting possibilities that are unlikely to occur.

¹Applied Research Team, Five AI, Edinburgh, United Kingdom. Correspondence: anthony.knittel@five.ai

²School of Informatics, University of Edinburgh, Edinburgh, United Kingdom

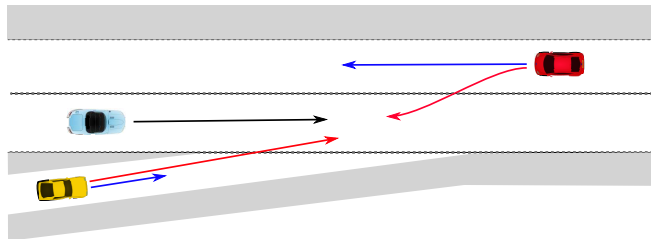


Fig. 1. Closest-mode evaluations are not sufficient for demonstrating usefulness. Only the closest modes are assessed (blue arrows), while additional modes (red arrows) can represent unreal and unlikely behaviours without affecting closest-mode scores. When mode probabilities are not used and not evaluated, these additional modes can interfere with ego planning (blue car).

Figure 1 shows an example where a predictor produces accurate predictions for each agent with the closest mode, while additional predictions conflict with preferred path of the ego vehicle. These predictions can cause the ego vehicle to avoid the expected conflicts, for example with rapid braking, even though they are unlikely to occur.

This problem can be addressed by a planner using the predicted probability of each mode. Probability estimates can be evaluated using measures such as predicted-mode RMS (predRMS), which evaluates mode probability estimates along with distances between predicted trajectories and observations. Existing methods such as [5], [6] have studied prediction using probabilistic predRMS evaluations on the NGSIM highway driving dataset [7].

Another limitation of typical closest-mode evaluations is that they compare trajectory positions without considering the distribution of predictions over space. Probability distributions are useful for a planner to estimate the probability that a region of space will be in conflict with other agents in the scene. Methods such as [8], [9] predict spatial distributions using a Gaussian Mixture Model (GMM), evaluated with the Negative-Log-Likelihood (NLL) of observations under the model, and are also studied on NGSIM.

Probabilistic evaluations and closest-mode evaluations can be viewed as analogous to precision and recall in binary classification (see Appendix), and provide complimentary evaluations that are more informative than either one alone. We argue that an effective predictor for interactive scenarios should be evaluated using both closest-mode and probabilistic measures. This is a challenging task as different evaluation measures produce different prediction strategies. Closest-mode evaluations (eg minADE/FDE/MR) favour diverse predictions, while probabilistic evaluations (predRMS, NLL) favour conservative predictions close to the mean

of expected behaviours, where the cost of predicting an incorrect mode is minimised.

To that end, we present DiPA (Diverse and Probabilistically Accurate prediction) – a method that achieves good scores on both closest-mode and probabilistic measures, by producing a diverse set of predictions with accurate mode probability estimates. We show that our method produces state-of-the-art predictions using minADE/minFDE/MR on INTERACTION, produces state-of-the-art predictions using predRMS/NLL on NGSIM [7], and improves over Multiple-Futures Prediction (MFP) [9] (and a variation thereof¹) when using both minADE/minFDE/MR and predRMS/NLL together on NGSIM and INTERACTION.

Beyond highlighting the importance of evaluating predictors with both closest-mode and probabilistic evaluations for interactive prediction, the key contributions of this work are: 1) a prediction architecture with a flexible representation that processes agent interactions in wide-ranging road layouts, and produces high accuracy predictions on interactive scenarios, 2) a training regime that supports a diverse set of predicted modes using a GMM-based spatial distribution, with accurate probability estimates that improves over existing methods, and 3) a revision to existing NLL measures to correct for current limitations.

II. EXISTING METHODS

Interactive prediction has been approached in different ways. Goal-based methods [10], [11], [12], [13], [14] identify a number of potential future targets that each agent may be heading towards, determine likelihoods of each, and produce predicted trajectories towards those goals. Flash [6] uses a combination of Bayesian inverse-planning and mixture-density networks to produce accurate predictions of trajectories in highway driving scenarios. Goal-based methods have the advantage of using the map to inform trajectory generation, and can use kinematically-sound trajectory generators. However, this can lead to limited diversity on other factors such as motion profile and path variations compared to data-driven methods.

Graph-based methods [15], [4], [2] combine map information and agent positions into a common representation, commonly processed with a graph neural-network in an encoder-decoder framework. Jia et al. [16] extend a graph-based model to consider the scene from each agent’s point of view rather than using a single central agent, and recurse each agent’s model of other agent behaviours. In general, graph-based methods allow encoding static layout of the scene and various agents in a generalisable way, and have shown good results on closest-mode prediction.

Regression-based methods use representations that directly map observations to predicted outputs. SAMMP [8] produces joint predictions of the spatial distribution of vehicles, using a multi-head self-attention function to capture interactions

between agents. Multiple-Futures Prediction (MFP) [9] models the joint futures of a number of interacting agents, with a number of learnt latent variables that are used for generating predicted future modes. Mersch et al. [17] present a temporal-convolution method for predicting interacting vehicles in a highway scenario where neighbouring agents are assigned specific roles based on relative positions to a central agent. These regression-based methods can be fast and accurate, but may have limited generalisability to different layouts when role-based representation of inputs is used.

The importance of balancing prediction diversity and accuracy has been recognised in [8] which trains a GMM model with NLL loss and shows improved diversity against prior art measured by MR. Rhinehart et al. [18] examined the generation of paths that are both diverse, to cover instances in the dataset, and precise, to minimise inconsistency with the data, using a specific cross-entropy term per objective. This balance is also addressed in generative CVAE models such as [19] which uses a trajectory sampler trained to extract diverse and plausible samples generated by the model.

To address the limitations of closest-mode and mean evaluation measures, [18] propose the use of information-based cross-entropy evaluations. The importance of evaluating with both displacement-error and NLL-based evaluations has also been recognised by [20], for evaluating trajectories produced by a generative model. Measures of diversity and precision have also been explored by [21] using closest-mode and mean mode evaluations, performed on joint predictions of various agents in a scene. A limitation of this approach is the lack of probabilistic weighting of predicted modes.

Existing models using the INTERACTION dataset have demonstrated good results on closest-mode evaluations (minADE/FDE/MR) [2], [3], [4], while models using NGSIM have shown good results on probabilistic evaluations (predRMS, NLL) [8], [17], [9], [6]. The joint task of producing diverse predictions at the same time as maintaining good probabilistic accuracy has generally not been addressed with interactive prediction. We demonstrate that the proposed DiPA method addresses this joint task, in a generalisable way that can be applied to the various scenes of interactive scenarios.

III. PROPOSED METHOD

DiPA uses an encoder-decoder architecture to produce multi-modal predictions, where each mode is represented by a sequence of spatial distributions modelled as a GMM. It is designed to handle a wide range of scenarios including roundabouts, junctions, highways and other road topologies with a varying numbers of agents in diverse arrangements. Predictions are performed for a specified prediction agent, which is evaluated for scoring, with a number of surrounding agents. Each of the agents are treated as symmetric entities in an unordered set with no need to assign specific roles based on relative positions. This allows flexible comparisons between agents to be performed and enables generalisability to different road layouts.

¹In order to compare with MFP on INTERACTION, we modify it to operate on more varied road scenarios, where originally it has been developed for highway driving with NGSIM. See Section IV-A

In contrast, MFP [9] uses a combination of posterior and predicted distribution weights for training the GMM, which has a tendency to produce a single dominant mode.

1) *Spatial distribution training*: The spatial distribution loss minimises the NLL score of an observation x under the predicted model, weighted by the training mode distribution W_r . This trains the parameters of the normal distribution μ, Σ , while W_r is constant. The loss is averaged over timesteps as shown in (4).

$$\mathcal{L}_{spatial} = -\frac{1}{T} \sum_t \ln \left(\sum_m W_{r,m} \mathcal{N}(x, \mu_{m,t}, \Sigma_{m,t}) \right) \quad (4)$$

The training weight distribution W_r emphasises training parameters of modes similar to the observation, supporting mode diversity, in contrast to standard NLL training based on the predicted mode weight distribution.

2) *Mode weight estimation training*: Two terms representing the predicted mode weights are produced by the model, W_s and W_n , which are based on similarity between predicted trajectory positions and observations, and low spatial distribution error, respectively. The preferred mode weighting for each objective can be inconsistent, resulting in the use of independent mode weight predictions. The trajectory-based mode estimation weight W_s is trained with a MSE-based loss that minimises the weighted MSE score, as shown in (5). With this loss W_s is trained while μ is constant.

$$\mathcal{L}_{MSE} = \sum_m W_{s,m} \frac{1}{T} \sum_t \|x_t - \mu_{m,t}\|^2 \quad (5)$$

The spatial distribution mode weight W_n is trained using two loss terms, a NLL-based loss that minimises the NLL score, and a training-weight loss that trains W_n to be similar to the training mode distribution W_r . The NLL-based mode loss is shown in (6), where W_n is trained and μ, Σ are constant.

$$\mathcal{L}_{NLL} = -\frac{1}{T} \sum_t \ln \left(\sum_m W_{n,m} \mathcal{N}(x, \mu_{m,t}, \Sigma_{m,t}) \right) \quad (6)$$

The training-weight loss minimises the Kullback-Leibler divergence between W_r and W_n , as shown in (7), where W_n is trained and W_r is constant.

$$\mathcal{L}_{KL} = D_{KL}(W_r || W_n) \quad (7)$$

The two mode estimation distributions W_s and W_n are based on different objectives, and favour RMS-based and NLL evaluations respectively. In order to produce a single prediction output that balances these objectives, a weighted average is returned $W_o = (1 - k_n)W_s + k_nW_n$, using $k_n = 0.9$, which has been chosen experimentally as shown in Section V-A.

IV. EXPERIMENTS

Experiments are conducted on the INTERACTION [1] and NGSIM [7] datasets to compare existing benchmarks against prior methods, and to compare both closest-mode and

probabilistic prediction of the proposed DiPA method against a baseline based on Multiple-Futures Prediction (MFP) [9].

1) *NGSIM dataset*: The NGSIM source dataset contains trajectory tracks for agents in two scenes (US-101 and I-80), and agents are assigned to train/evaluation splits based on vehicle identifier, as used in [5]. Instances are created based on a central agent, for each fully-observed window of 8 seconds (3 observed and 5 future). For each instance up to 20 neighbouring agents are also observed, while agents that have been assigned to different splits are not used for training.

2) *INTERACTION dataset*: The single-agent INTERACTION dataset [1] is divided into instances based on each fully-observed agent in each case window, with a 4 second duration. Prediction is performed using a 1 second observed period and 3 second prediction period.

On both datasets global coordinates are used. Pre-processing centers units on the last observed position of the agent to be predicted, with rotation such that the yaw of the prediction agent is zero (at the last observed timestep).

A. Revised implementation of Multiple-Futures Prediction

MFP [9] is a useful baseline as it is an accurate method based on a GMM, allowing comparison on each of the evaluation measures. A limitation of MFP is that it has been implemented using local lane-based coordinates, which are suitable for highway driving involving mostly parallel lanes. This representation is not directly generalisable to more complex scenarios involving intersections, roundabouts and other non-parallel topology.

Experiments on INTERACTION require global coordinates, and to examine the effect of changing from local to global coordinates we implement a global coordinate approach on NGSIM (*MFP-global*). For consistency with local coordinates, each instance is re-framed to be centered on the last observed position and rotated on the orientation of the central agent. A revised neighbour grid is used to run MFP on INTERACTION, which includes more varied road topologies than NGSIM. MFP represents neighbours using a 13×3 grid of positions in the central and neighbouring lanes, based on distances from the central agent. A comparable neighbour grid is produced based on the central and neighbouring lane patches corresponding with the central agent. All following and preceding lane patches from the central lane patch(es) represent the central lane, and similarly for the neighbouring lanes. Grid spacing distances for each neighbour agent are found based on the nearest midline path, using the progress distance of the neighbour agent relative to the central agent to define the position in the neighbour grid. This defines a neighbour grid similar to that used in MFP, and implements the *MFP-Lanelet2* method (also using global coordinates).

B. Evaluation methods

We evaluate with NLL, predRMS, minADE, minFDE and Miss-Rate (MR) measures, defined as follows.

1) *predRMS*: the root-mean-square (RMS) error of the most probable predicted mode is calculated for a number of timesteps, over the set of instances of the dataset ($1 \leq n \leq N$) as shown in (8), where μ_i is the predicted position for the most probable mode $i = \arg \max_m(W_m)$ as used in [5], [9], [6]:

$$\text{predRMS}_t = \sqrt{\frac{1}{N} \sum_{n=1}^N \|x_{n,t} - \mu_{i,t}\|^2} \quad (8)$$

Previously reported methods have used different numbers of modes, including different numbers of modes on different instances of a dataset. Experiments reported here use a fixed number of modes, with the same number specified for minADE/minFDE evaluations. The number of modes used is not an inherent property of the evaluation measure.

2) *Minimum average displacement error (minADE)*: evaluates the average Euclidian distance between the closest predicted trajectory mode and the ground truth over a horizon (T), while the *minimum final displacement error (minFDE)* uses the closest final position, as follows.

$$\text{minADE} = \min_m \left(\frac{1}{T} \sum_{t=1}^T \|x_t - \mu_{t,m}\| \right) \quad (9)$$

$$\text{minFDE} = \min_m (\|x_T - \mu_{T,m}\|) \quad (10)$$

The number of modes used strongly affects the evaluation result, and is reported with the evaluation.

3) *Miss-rate*: is defined as the percentage of instances where the minimum spatial error on the final timestep is larger than a given threshold, ie $\text{minFDE} > k \in \mathbb{R}$. We use a threshold of $k = 2m$ as used in [10], [8].

4) *Negative-log-likelihood (NLL)*: describes the log-probability of observed instances over a predicted distribution. Previous methods [9], [24], [8] have used a GMM representation, although NLL is a general property that can be compared between different representations. NLL evaluates how probable an observed event was predicted to occur, a good model will assign high probability to each observed event, resulting in a low NLL score. Calculation of the NLL score using a GMM is shown in (11). This is represented using a center position $\mu_m \in \mathbb{R}^2$, covariance matrix $\Sigma_m \in \mathbb{R}^{2 \times 2}$ and mode weight $W_m \in \mathbb{R}$ for each predicted mode, where $x \in \mathbb{R}^2$ is the ground-truth position. This is determined for each timestep of the prediction, and averaged over timesteps.

$$\text{NLL} = \frac{1}{T} \sum_{t=1}^T -\ln \left(\sum_{m=1}^M W_m \mathcal{N}(x_t, \mu_{m,t}, \Sigma_{m,t}) \right)$$

$$\mathcal{N}(x, \mu, \Sigma) = \frac{1}{2\pi \sqrt{|\Sigma|}} e^{-\frac{1}{2}(x-\mu)^T \Sigma^{-1}(x-\mu)} \quad (11)$$

NLL as a concept is a dimensionless property, however previous results and the evaluation in 11 are based on probability density, without reducing to a dimensionless value. Observed samples are defined as points, which have

zero probability in a spatial distribution as a result of being a position with no size. It is possible to produce a probability evaluation using an area instead of a point, however the area to use is not well defined or meaningful for the task. As dimensioned probability density values are used, and the NLL measure is determined from this value, it is important to record the dimensions of the density-based NLL property reported. Previous methods have used inconsistent units, in feet [9] and in meters [8], so to address this problem we present units of measurement with reported results.

Another limitation is that in existing definitions NLL is an unbounded quantity, which allows scores on a small number of instances to greatly influence evaluation on the dataset. This is both a theoretical and a practical problem, as for example a dataset may contain a stationary object, where the center of a predicted GMM can be accurately chosen, and the distribution width reduced to an arbitrarily high density, bounded only by numerical limits. When represented with a 64-bit float (with limit 5.5×10^{-309}), this can result in a NLL score of -710 for a single instance.

We suggest that a maximum probability density be applied, as for vehicle prediction there is no practical advantage in distinguishing between very tight bounds. Mercat et al. [8] apply a minimum limit to the standard deviation of $\sigma = 0.1m$, for the purposes of avoiding overfitting. This is a useful minimum value, and we believe that there is no meaningful advantage of predicting with a higher probability density than this in the context of vehicle prediction, while narrower bounds can change the scores substantially. We extend the definition to apply to evaluation, where the probability density is capped for each instance, based on the maximum probability density of a normal distribution with $\sigma = 0.1m$, which is $\frac{1}{2\pi \cdot 0.1^2} m^{-2}$ (approx. $15.92m^{-2}$), and minimum NLL score of $-\ln(\frac{1}{2\pi \cdot 0.1^2})$ (approx. -2.77). This can be used with any probability distribution, including GMMs and raster-based representations.

V. RESULTS

Results of experiments on NGSIM using the predRMS evaluation are shown in Table I. Values above the single line are previously reported, below the line are newly calculated, and ablations are shown below the double line. New results are shown using the same experiment for all evaluations, while separate specialised experiments may have been used with previous methods. DiPA improves over previous methods on predRMS evaluations, which requires generating a set of predicted trajectories and accurately predicting the most probable mode. Results with the revised MFP-global method show it is able to operate similar to the original implementation with slightly higher error. Evaluation of the spatial distribution using NLL evaluations are shown in Table II, showing DiPA produces more accurate probabilistic predictions than previous methods. NLL results for generated runs (below single line) are reported with the thresholded NLL score described in Section IV-B.4 (thresholding does not give an advantage). Miss-Rate (MR) results have been shown on previous methods such as SAMMP [8] that use

TABLE I
PROBABILISTIC PREDRMS SCORES ON NGSIM

Method	predRMS (by time period) [m]				
	1s	2s	3s	4s	5s
CV [25]	0.76	1.82	3.17	4.80	6.70
CSP(M) [5], [8]	0.59	1.27	2.13	3.22	4.64
GRIP [26] ²	0.52	1.22	2.05	3.13	4.47
SAMMP [8]	0.51	1.13	1.88	2.81	3.98
Flash [6]	0.51	1.15	1.84	2.64	3.62
MFP [9]	0.54	1.17	1.87	2.71	3.67
MFP-global	0.64	1.31	2.16	3.21	4.46
DiPA	0.46	1.04	1.70	2.47	3.43
Trajectory mode weight	0.46	1.04	1.70	2.45	3.39
Spatial mode weight	0.47	1.08	1.79	2.62	3.64
Standard NLL loss	0.44	1.03	1.66	2.48	3.50
Closest-mode training	0.43	0.99	1.64	2.44	3.43
Posterior training	0.43	0.99	1.65	2.47	3.50

TABLE II
PROBABILISTIC NLL SCORES ON NGSIM (MODES=5)

Method	NLL (by time period) [$\ln m^{-2}$]				
	1s	2s	3s	4s	5s
CV [25]	0.82	2.32	3.23	3.91	4.46
CSP(M) [5], [8]	-0.41	1.07	1.93	2.55	3.08
SAMMP [8]	-0.36	0.70	1.51	2.13	2.64
MFP [9]	-0.64	0.71	1.56	2.21	2.74
MFP-global	-0.55	0.96	1.84	2.50	3.03
DiPA	-1.22	0.20	1.23	2.01	2.61
Trajectory weight	9810.85	3670.04	63.28	29.92	17.52
Spatial weight	-1.24	0.18	1.21	2.00	2.60
Standard NLL loss	-1.36	0.06	1.11	1.91	2.60
Closest-mode	-1.17	0.51	1.60	2.36	2.86
Posterior training	-1.30	0.11	1.16	1.95	2.60

standard NLL training, as shown in the closest-mode evaluations in Table III. DiPA shows improved MR evaluation, indicating improved ability to produce diverse modes that closely cover instances of the dataset.

Results of experiments on INTERACTION using the standard closest-mode evaluations is shown in Table IV, showing that DiPA produces lower error predictions based on the closest mode than the comparison methods. This shows that the model produces a diverse set of predicted trajectories, that accurately capture specific behaviours observed in the INTERACTION dataset.

Multiple evaluation measures are compared from the same run on NGSIM in Tables I, II, III below the single line. These show that the baseline MFP methods produce accurate probabilistic predictions as measured with predRMS and NLL, however show relatively high error on the minADE/FDE evaluations. This suggests limited diversity of predictions, which limits the ability to closely match individual instances. DiPA is able to produce good scores on both types of evaluation, indicating it is able to capture both diverse and probabilistically accurate predictions on NGSIM.

Comparison of multiple evaluations on INTERACTION (Tables IV, V, VI below the single line) also shows improved results with DiPA against *MFP-Lanelet2* on all evaluation measures. *MFP-Lanelet2* has shown the ability to generalise

TABLE III
CLOSEST-MODE SCORES ON NGSIM

Method	minADE ₅	minFDE ₅	MR ₅
CV [25]	-	-	0.71
CSP(M) [5], [8]	-	-	0.44
SAMMP [8]	-	-	0.23
MFP [9]	1.07	2.15	0.40
MFP-global	1.17	2.44	0.43
DiPA	0.48	0.86	0.07
Trajectory mode weight	0.48	0.86	0.07
Spatial mode weight	0.48	0.86	0.07
Standard NLL loss	0.90	1.75	0.32
Closest-mode training	0.46	0.82	0.05
Posterior training	0.51	0.99	0.16

TABLE IV
CLOSEST-MODE SCORES ON INTERACTION (MODES=6)

Method	minADE ₆	minFDE ₆	MR ₆
TNT [10]	0.21	0.67	-
ReCoG [15]	0.19	0.66	-
ITRA [3]	0.17	0.49	-
GoHome [4]	-	0.45	-
StarNet [2] ^a	0.16	0.49	-
joint-StarNet [2] ^a	0.13	0.38	-
MFP-Lanelet2	0.43	1.20	0.19
DiPA	0.11	0.34	0.02
Trajectory mode weight	0.11	0.34	0.02
Spatial mode weight	0.11	0.34	0.02
Standard NLL loss	0.18	0.47	0.03
Closest-mode training	0.11	0.33	0.01
Posterior training	0.11	0.36	0.02

^aThis is run with a 2.5 second observed window instead of 1 second

MFP to operate on the wide range of scenarios present in the INTERACTION dataset. DiPA uses a more general input representation than the grid representation used by MFP, allowing flexible use on different scenarios. Overall DiPA has shown good results for producing diverse predictions that capture instances in the dataset (on minADE/FDE/MR scores), while also showing high probabilistic prediction accuracy on predRMS and NLL evaluations.

Figure 3 shows selected instances from the INTERACTION dataset, representing behaviours exhibited by DiPA.

A. Ablation study

Experiments using variations of the DiPA model are shown in each result table below the double line. Use of the *trajectory mode weight* W_s alone ($k_n = 0$) favours RMS scores at a cost of NLL evaluations, while use of the *spatial mode weight* W_n ($k_n = 1$) produces lower NLL error with increased RMS errors. The effect of changing the proportion k_n is shown in Figure 4, showing values for the final timestep. A proportion of $k_r = 0.9$ has been chosen to provide a balanced result.

Standard NLL loss shows a condition where training is performed directly from the NLL loss, using the predicted

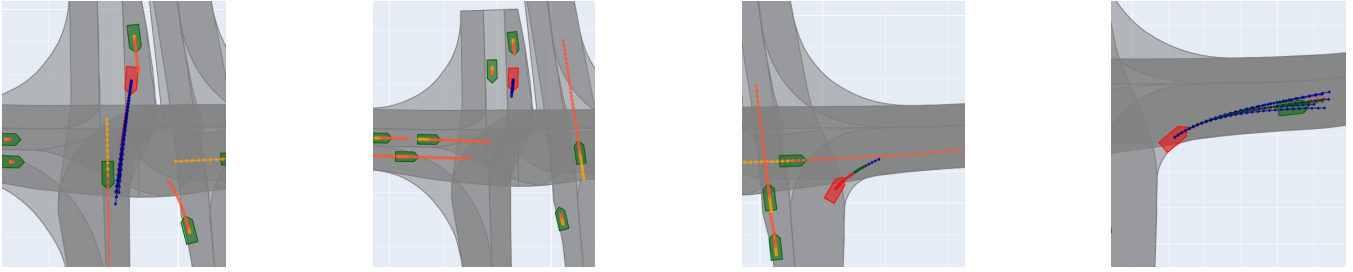


Fig. 3. Qualitative results, showing (from L-R) 1. the predicted agent entering the intersection when crossing vehicles are slow and 2. yielding to crossing vehicles when there is not enough room to pass. 3. prediction of slow movement to merge behind the faster vehicle, showing diversity over speeds for predicted modes and 4. merging at higher speed when clear, and showing diversity over predicted paths.

TABLE V
PROBABILISTIC PREDRMS SCORES ON INTERACTION

Method	predRMS [m]		
	1s	2s	3s
MFP-Lanelet2	0.21	0.95	2.37
DiPA	0.11	0.47	1.28
Trajectory mode weight	0.11	0.47	1.25
Spatial mode weight	0.12	0.51	1.38
Standard NLL loss	0.11	0.44	1.18
Closest-mode training	0.15	0.50	1.28
Posterior training	0.10	0.46	1.27

TABLE VI
PROBABILISTIC NLL SCORES ON INTERACTION (MODES=6)

Method	NLL [$\ln m^{-2}$]		
	1s	2s	3s
MFP-Lanelet2	-1.87	0.46	2.17
DiPA	-2.09	-0.85	0.76
Trajectory mode weight	93.20	18.19	12.79
Spatial mode weight	-2.10	-0.87	0.76
Standard NLL loss	-2.27	-0.58	0.95
Closest-mode training	-1.56	-0.87	0.73
Posterior training	-2.22	-0.94	0.70

mode distribution as the training weights. This shows lower error on NLL, but substantially higher error on closest-mode evaluations, showing that it is not able to capture specific behaviour modes as well. *Closest-mode training* based on the mode weight W_c only ($k_r = 0$) shows lower closest-mode errors but higher NLL error on NGSIM, which contains more noise than INTERACTION. During development we have found that using W_c only can lead to one or a few modes dominating, and is expected to be sensitive to initialisation. *Posterior training* based on W_p shows higher closest-mode but lower predRMS and NLL error. A balanced setting ($k_r = 0.5$) provides a balanced, reliable approach that improves over prior methods on all measures.

VI. SUMMARY

A practical predictor to support an autonomous vehicle in interactive scenarios should produce diverse predictions that capture distinct modes of behaviour that agents may follow, and predict the probability that each may occur. A limitation of previous predictors is that they have demonstrated diverse

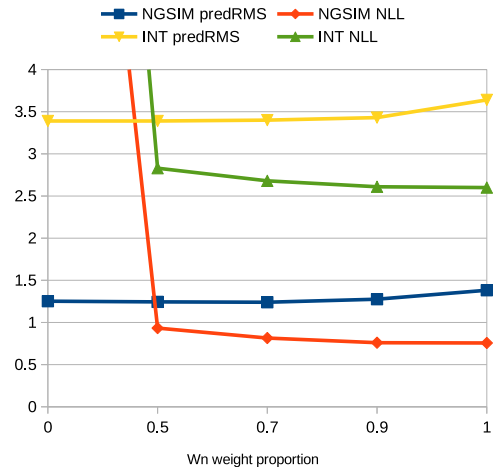


Fig. 4. Effect of mode weighting between trajectory- and spatial-distribution-based weights.

predictions without capturing probabilities of the various modes (e.g. on INTERACTION), or have shown accurate probabilistic estimates without demonstrated capturing of distinct behaviours (e.g. on NGSIM).

The proposed method has the ability to both capture diverse predictions on INTERACTION with lower minADE/FDE error than previous methods, and produce accurate probabilistic predictions on NGSIM that improve on previous methods based on predRMS and NLL. Comparing both diversity and probabilistic evaluation together also shows improvement over the MFP baseline, on each of the evaluation measures.

This demonstrates that DiPA produces multi-modal predictions that capture a diverse range of expected behaviours, along with accurate mode probability and spatial distribution estimates. This allows a planner to assess the risk of conflict for different possible plans for the ego vehicle, addressing the limitation where previous interactive predictors can produce additional unlikely mode predictions that can interfere with planning, as shown in Figure 1.

DiPA uses a flexible representation of observed agents that does not require role assignment, and is based on versatile pair-wise comparisons to capture interactions between agents in the scene, allowing generalisability for operating on dif-

ferent scenarios with widely varying road layouts.

REFERENCES

- [1] W. Zhan, L. Sun, D. Wang, H. Shi, A. Clause, M. Naumann, J. Kummerle, H. Konigshof, C. Stiller, A. de La Fortelle, *et al.*, “Interaction dataset: An international, adversarial and cooperative motion dataset in interactive driving scenarios with semantic maps,” *arXiv preprint arXiv:1910.03088*, 2019.
- [2] F. Janjoš, M. Dolgov, and J. M. Zöllner, “StarNet: Joint action-space prediction with star graphs and implicit global frame self-attention,” *arXiv preprint arXiv:2111.13566*, 2021.
- [3] A. Ścibior, V. Lioutas, D. Reda, P. Bateni, and F. Wood, “Imagining the road ahead: Multi-agent trajectory prediction via differentiable simulation,” in *2021 IEEE International Intelligent Transportation Systems Conference (ITSC)*. IEEE, 2021, pp. 720–725.
- [4] T. Gilles, S. Sabatini, D. Tshikhou, B. Stanculescu, and F. Moutarde, “GoHome: Graph-oriented heatmap output for future motion estimation,” *arXiv preprint arXiv:2109.01827*, 2021.
- [5] N. Deo and M. M. Trivedi, “Convolutional social pooling for vehicle trajectory prediction,” in *IEEE Conference on Computer Vision and Pattern Recognition Workshops*, 2018, pp. 1468–1476.
- [6] M. Antonello, M. Dobre, S. V. Albrecht, J. Redford, and S. Ramamoorthy, “Flash: Fast and light motion prediction for autonomous driving with Bayesian inverse planning and learned motion profiles,” *arXiv preprint arXiv:2203.08251*, 2022.
- [7] J. Colyar and J. Halkias, “Next generation simulation (NGSIM) vehicle trajectories and supporting data,” 2016. [Online]. Available: <http://doi.org/10.21949/1504477>
- [8] J. Mercat, T. Gilles, N. El Zoghby, G. Sandou, D. Beauvois, and G. P. Gil, “Multi-head attention for multi-modal joint vehicle motion forecasting,” in *2020 IEEE International Conference on Robotics and Automation (ICRA)*. IEEE, 2020, pp. 9638–9644.
- [9] C. Tang and R. R. Salakhutdinov, “Multiple Futures Prediction,” *Advances in Neural Information Processing Systems*, vol. 32, 2019.
- [10] H. Zhao, J. Gao, T. Lan, C. Sun, B. Sapp, B. Varadarajan, Y. Shen, Y. Shen, Y. Chai, C. Schmid, *et al.*, “TNT: Target-driven trajectory prediction,” *arXiv preprint arXiv:2008.08294*, 2020.
- [11] J. Gu, C. Sun, and H. Zhao, “DenseTNT: End-to-end trajectory prediction from dense goal sets,” in *IEEE/CVF International Conference on Computer Vision*, 2021, pp. 15 303–15 312.
- [12] J. P. Hanna, A. Rahman, E. Fosong, F. Eiras, M. Dobre, J. Redford, S. Ramamoorthy, and S. V. Albrecht, “Interpretable goal recognition in the presence of occluded factors for autonomous vehicles,” in *IEEE/RSJ International Conf. on Intelligent Robots and Systems*, 2021.
- [13] S. V. Albrecht, C. Brewitt, J. Wilhelm, B. Gyevnar, F. Eiras, M. Dobre, and S. Ramamoorthy, “Interpretable goal-based prediction and planning for autonomous driving,” in *IEEE International Conference on Robotics and Automation (ICRA)*, 2021.
- [14] C. Brewitt, B. Gyevnar, S. Garcin, and S. V. Albrecht, “GRIT: fast, interpretable, and verifiable goal recognition with learned decision trees for autonomous driving,” in *IEEE/RSJ International Conference on Intelligent Robots and Systems (IROS)*, 2021.
- [15] X. Mo, Y. Xing, and C. Lv, “ReCog: A deep learning framework with heterogeneous graph for interaction-aware trajectory prediction,” *arXiv preprint arXiv:2012.05032*, 2020.
- [16] X. Jia, L. Sun, H. Zhao, M. Tomizuka, and W. Zhan, “Multi-agent trajectory prediction by combining egocentric and allocentric views,” in *Conference on Robot Learning*. PMLR, 2022, pp. 1434–1443.
- [17] B. Mersch, T. Höllen, K. Zhao, C. Stachniss, and R. Roscher, “Maneuver-based trajectory prediction for self-driving cars using spatio-temporal convolutional networks,” in *IEEE/RSJ International Conf. on Intelligent Robots and Systems*. IEEE, 2021, pp. 4888–4895.
- [18] N. Rhinehart, K. M. Kitani, and P. Vernaza, “R2p2: A reparameterized pushforward policy for diverse, precise generative path forecasting,” in *European Conference on Computer Vision*, 2018, pp. 772–788.
- [19] Y. Yuan, X. Weng, Y. Ou, and K. M. Kitani, “Agentformer: Agent-aware transformers for socio-temporal multi-agent forecasting,” in *Proceedings of the IEEE/CVF International Conference on Computer Vision*, 2021, pp. 9813–9823.
- [20] T. Salzmann, B. Ivanovic, P. Chakravarty, and M. Pavone, “Trajectron++: Dynamically-feasible trajectory forecasting with heterogeneous data,” in *European Conference on Computer Vision*. Springer, 2020, pp. 683–700.
- [21] S. Casas, C. Gulino, S. Suo, K. Luo, R. Liao, and R. Urtasun, “Implicit latent variable model for scene-consistent motion forecasting,” in *European Conference on Computer Vision*. Springer, 2020, pp. 624–641.
- [22] J. Zhou, G. Cui, S. Hu, Z. Zhang, C. Yang, Z. Liu, L. Wang, C. Li, and M. Sun, “Graph neural networks: A review of methods and applications,” *AI Open*, vol. 1, pp. 57–81, 2020.
- [23] C. R. Qi, H. Su, K. Mo, and L. J. Guibas, “Pointnet: Deep learning on point sets for 3d classification and segmentation,” in *IEEE conference on computer vision and pattern recognition*, 2017, pp. 652–660.
- [24] H. Song, W. Ding, Y. Chen, S. Shen, M. Y. Wang, and Q. Chen, “PiP: Planning-informed trajectory prediction for autonomous driving,” in *European Conference on Computer Vision*. Springer, 2020, pp. 598–614.
- [25] J. Mercat, N. E. Zoghby, G. Sandou, D. Beauvois, and G. P. Gil, “Kinematic single vehicle trajectory prediction baselines and applications with the NGSIM dataset,” *arXiv preprint arXiv:1908.11472*, 2019.
- [26] X. Li, X. Ying, and M. C. Chuah, “Grip: Graph-based interaction-aware trajectory prediction,” in *2019 IEEE Intelligent Transportation Systems Conference (ITSC)*. IEEE, 2019, pp. 3960–3966.

APPENDIX

RELATIONSHIP BETWEEN PROBABILISTIC / CLOSEST-MODE EVALUATIONS AND PRECISION / RECALL

In binary classification, recall refers to the proportion of true positives covered by predictions, and precision refers to the proportion of true positives among predicted positives. High recall requires capturing each positive instance, while high precision requires only predicting positive instances that occur and minimising false positive predictions.

Predicted trajectories are evaluated based on distances with ground-truth trajectory instances, however there are correspondences with precision and recall. Closest-mode evaluations such as minADE/FDE evaluate whether instances in a dataset are captured by at least one of the predicted modes, which is related to recall. Real-valued minADE/FDE measures can be converted to binary recall by measuring the proportion of instances where at least one predicted mode is within a given distance threshold of the ground-truth.

Probabilistic measures such as predRMS (8) and other weighted RMS measures are related to precision. An important concept that is measured with precision, is the presence of false-positive predictions. In the case of trajectory prediction, predictions that are not similar to an observed instance, and have also been assigned high probability mass, are related to false-positives. Predictions with mode probabilities can be converted to binary precision using a threshold of mode probability to select which modes are being predicted, or in the case of predRMS, selecting only the most probable prediction. A distance threshold then determines which predicted modes are close to an observed instance, and the ratio of close predicted modes with all predicted modes corresponds with binary precision.

Precision and recall are complimentary measures of a binary classifier, and in the same way closest-mode and probabilistic evaluations are complementary and important measures of trajectory prediction.